Klastomycter conodentatus, gen et sp. nov., a small early Permian parareptile with conical teeth from Richards Spur, Oklahoma (#101822)

First submission

Guidance from your Editor

Please submit by 10 Jul 2024 for the benefit of the authors (and your token reward) .



Structure and Criteria

Please read the 'Structure and Criteria' page for guidance.



Custom checks

Make sure you include the custom checks shown below, in your review.



Author notes

Have you read the author notes on the guidance page?



Raw data check

Review the raw data.



Image check

Check that figures and images have not been inappropriately manipulated.

If this article is published your review will be made public. You can choose whether to sign your review. If uploading a PDF please remove any identifiable information (if you want to remain anonymous).

Files

Download and review all files from the <u>materials page</u>.



Custom checks

7 Figure file(s)

New species checks

Have you checked our <u>new species policies</u>?

Do you agree that it is a new species?

Is it correctly described e.g. meets ICZN standard?

Structure and Criteria



Structure your review

The review form is divided into 5 sections. Please consider these when composing your review:

- 1. BASIC REPORTING
- 2. EXPERIMENTAL DESIGN
- 3. VALIDITY OF THE FINDINGS
- 4. General comments
- 5. Confidential notes to the editor
- You can also annotate this PDF and upload it as part of your review

When ready submit online.

Editorial Criteria

Use these criteria points to structure your review. The full detailed editorial criteria is on your guidance page.

BASIC REPORTING

- Clear, unambiguous, professional English language used throughout.
- Intro & background to show context.
 Literature well referenced & relevant.
- Structure conforms to <u>PeerJ standards</u>, discipline norm, or improved for clarity.
- Figures are relevant, high quality, well labelled & described.
- Raw data supplied (see <u>PeerJ policy</u>).

EXPERIMENTAL DESIGN

- Original primary research within Scope of the journal.
- Research question well defined, relevant & meaningful. It is stated how the research fills an identified knowledge gap.
- Rigorous investigation performed to a high technical & ethical standard.
- Methods described with sufficient detail & information to replicate.

VALIDITY OF THE FINDINGS

- Impact and novelty is not assessed.

 Meaningful replication encouraged where rationale & benefit to literature is clearly stated.
- All underlying data have been provided; they are robust, statistically sound, & controlled.



Conclusions are well stated, linked to original research question & limited to supporting results.

Standout reviewing tips



The best reviewers use these techniques

Τ	p

Support criticisms with evidence from the text or from other sources

Give specific suggestions on how to improve the manuscript

Comment on language and grammar issues

Organize by importance of the issues, and number your points

Please provide constructive criticism, and avoid personal opinions

Comment on strengths (as well as weaknesses) of the manuscript

Example

Smith et al (J of Methodology, 2005, V3, pp 123) have shown that the analysis you use in Lines 241-250 is not the most appropriate for this situation. Please explain why you used this method.

Your introduction needs more detail. I suggest that you improve the description at lines 57-86 to provide more justification for your study (specifically, you should expand upon the knowledge gap being filled).

The English language should be improved to ensure that an international audience can clearly understand your text. Some examples where the language could be improved include lines 23, 77, 121, 128 – the current phrasing makes comprehension difficult. I suggest you have a colleague who is proficient in English and familiar with the subject matter review your manuscript, or contact a professional editing service.

- 1. Your most important issue
- 2. The next most important item
- 3. ...
- 4. The least important points

I thank you for providing the raw data, however your supplemental files need more descriptive metadata identifiers to be useful to future readers. Although your results are compelling, the data analysis should be improved in the following ways: AA, BB, CC

I commend the authors for their extensive data set, compiled over many years of detailed fieldwork. In addition, the manuscript is clearly written in professional, unambiguous language. If there is a weakness, it is in the statistical analysis (as I have noted above) which should be improved upon before Acceptance.



Klastomycter conodentatus, gen et sp. nov., a small early Permian parareptile with conical teeth from Richards Spur, Oklahoma

Robert R Reisz Corresp., 1, 2, Dylan CT Rowe Corresp., 1, 2, Joseph J Bevitt 3

Corresponding Authors: Robert R Reisz, Dylan CT Rowe Email address: robert.reisz@utoronto.ca, dylan.rowe@mail.utoronto.ca

A small, pristinely preserved specimen recently discovered from the Dolese Brothers limestone guarry near Richards Spur, Oklahoma provides evidence for the presence of a new early Permian parareptile at this locality. The specimen includes an articulated, nearly complete skull roof, and with the right premaxilla, right quadratojugal, most of the right palate, as well as the right epipterygoid and the sphenethmoid preserved inside. Although similar in many respects to the other contemporary parareptiles Acleistorhinus, Delorhynchus and Colobomycter, it can be distinguished from other acleistorhinids by the presence of a number of autapomorphies related to its dentition. Phylogenetic analysis places it closer to Delorhynchus and Colobomycter within Acleistorhinidae than to Acleistorhinus pteroticus. Unique aspects of the present specimen include the pronounced anterior extension of the lacrimal bone, largely homodont dentition composed of simple conical crowns with slight recurvature in the premaxillary and anterior maxillary teeth, and simple conical crowns in posterior maxillary dentition. The discovery of this new parareptile along with the surprisingly large number of acleistorhinids at Richards Spur highlights the importance of the unique fissure and vertical cave system at this site. No other early Permian site has provided such a wide diversity of parareptilian taxa, part of a complex community of terrestrial vertebrates. The present specimen highlights the fine niche partitioning that appears to have been present among reptiles of this region.

¹ Department of Biology, University of Toronto, Mississauga, Ontario, Canada

² Dinosaur Evolution Research Center, Jilin University ([[[[]]]]), Changchun, China

Australian Centre for Neutron Scanning, Australian Nuclear Science and Technology Organization, Sydney, New South Wales, Australia



- 1 Klastomycter conodentatus, gen et sp. nov., a small early Permian parareptile
- 2 with conical teeth from Richards Spur, Oklahoma
- 3 Robert R. Reisz^{1,2}, Dylan C. T. Rowe^{1,2} & Joseph J. Bevitt³
- 4 Department of Biology, University of Toronto, Mississauga, Mississauga, Ontario
- 5 ² Dinosaur Evolution Research Center, Jilin University, Changchun, China
- 6 ³ Australian Centre for Neutron Scanning, Australian Nuclear Science and Technology
- 7 Organization, Sydney, New South Wales, Australia

- 9 Corresponding Author:
- 10 Dylan Rowe^{1,2}
- 11 3359 Mississauga Road
- 12 Mississauga, ON L5L 1C6
- 13 Email Address: dylan.rowe@mail.utoronto.ca

14

15



17

19

21

25

27

29

31

Abstract

A small, pristinely preserved specimen recently discovered from the Dolese Brothers limestone guarry near Richards Spur, Oklahoma provides evidence for the presence of a new early Permian 18 parareptile at this locality. The specimen includes an articulated, nearly complete skull roof, and 20 with the right premaxilla, right quadratojugal, most of the right palate, as well as the right epipterygoid and the sphenethmoid preserved inside. Although similar in many respects to the other contemporary parareptiles Acleistorhinus, Delorhynchus and Colobomycter, it can be 22 distinguished from other acleistorhinids by the presence of a number of autapomorphies related 23 to its dentition. Phylogenetic analysis places it closer to Delorhynchus and Colobomycter within 24 Acleistorhinidae than to Acleistorhinus pteroticus. Unique aspects of the present specimen include the pronounced anterior extension of the lacrimal bone, largely homodont dentition 26 composed of simple conical crowns with slight recurvature in the premaxillary and anterior maxillary teeth, and simple conical crowns in posterior maxillary dentition. The discovery of this 28 new parareptile along with the surprisingly large number of acleistorhinids at Richards Spur highlights the importance of the unique fissure and vertical cave system at this site. No other 30 early Permian site has provided such a wide diversity of parareptilian taxa, part of a complex community of terrestrial vertebrates. The present specimen highlights the fine niche partitioning 32 33 that appears to have been present among reptiles of this region.

34 35

Introduction

36 37

38

39 40

41 42

43

44 45

46

47

48 49

50

51

52

53

54 55

56

The Dolese Brothers Limestone Quarry near Richards Spur, Oklahoma preserves a complex cave system that has yielded since the early 20th century a vast number of terrestrial tetrapod fossils dating back to the early Permian (289 Ma.) (MacDougall et al. 2017a). Over 30 taxa have been identified at this locality, making it the most taxonomically rich site for Paleozoic terrestrial tetrapods yet discovered (Sullivan et al., 2000; MacDougall et al. 2017). The fossil preservation observed at Richards Spur is, in part, a result of large crevices in the rock which were open to the ground surface during the Lower Permian (Olson, 1991). This vertical cave system was likely detrimental to many of the terrestrial tetrapods of the time, as the crevices could reach a depth of more than 30 metres (Olson, 1991; Sullivan et al., 2000). Remains of animals who either suffered a fatal accident, inhabited the areas around the openings of the crevices and were washed in by monsoonal rainfall or somehow ended up in the crevices by other means became preserved through geological time as clay and other Permian sediments filled the caves (Sullivan et al., 2000; MacDougall et al., 2017). This natural trap has allowed for the preservation of small Permian tetrapods in a way which has not been seen anywhere else. What were once large crevices often acting as natural traps for terrestrial vertebrates are now exposed to us as fissures at Richards Spur through excavations for the surrounding Ordovician limestone where the caves first developed (Sullivan et al., 2000; MacDougall et al., 2017).

Among the many terrestrial tetrapods found at Richards Spur are those belonging to Parareptilia, a group of enigmatic reptiles that were relatively rare during the early Permian but became very common towards the end of that period (Reisz et al., 2014). The importance of



- 57 Richards Spur cannot be overestimated as it has provided us with most of the early Permian
- 58 parareptiles that represent the initial stages of diversification of this clade. Genera found at
- 59 Richards Spur include two species of *Colobomycter*, three species of *Delorhynchus*,
- 60 Feeserpeton, Bolosaurus, Microleter and Abyssomedon (Vaughn, 1958; Fox, 1962; Daly, 1969;
- 61 Reisz et al., 2002; Tsuji et al., 2010; MacDougall & Reisz, 2012; Rowe et al., 2021). The
- 62 discovery of this small partial skull, which is described here, adds another genus to this list. This
- 63 fossil specimen includes an articulated skull roof and several palatal elements. The superficial
- 64 similarity of this specimen to that of *Acleistorhinus pteroticus*, a parareptile found at another
- locality in Oklahoma, provides support for the idea that this animal is an acleistorhinid (deBraga
- & Reisz, 1996). While these two specimens closely resemble one another at first glance, several
- 67 key features can be identified which support the identification of this parareptile as a new genus
- 68 separate from that of *Acleistorhinus pteroticus*.

Materials and Methods

70 71 72

73

74

76

77

78 79

80 81

82 83

84

85

86

87 88

89 90

91

92

93

94

95

96

97

69

Non-destructive, thermal-neutron microtomographic measurement of specimen

BMRP2008.3.3 was performed using the DINGO thermal neutron

radiography/tomography/imaging station, located at the 20 MW Open- Pool Australian

75 Lightwater (OPAL) reactor housed at the Australian Nuclear Science and Technology

Organisation (ANSTO), Lucas Heights, New South Wales, Australia.

For this study, DINGO was equipped with an Iris 15 sCMOS camera (16-bit, 5056×2960 pixels) coupled with a Makro Planar 100 mm Carl Zeiss lens and a 20 μ m thick terbium-doped Gadox scintillator screen (Gd2O2S:Tb, RC Tritec AG) to yield a pixel size of $14.5 \times 14.5 \mu$ m and field of view was of 43 x 73 mm². DINGO was operated in high-flux mode, with a collimation ratio (L/D) of 500 was used, where L is the neutron aperture-to-sample length and D is the neutron aperture diameter, supplying a flux at sample of $4.75 \times 107 n \cdot cm^{-2}s^{-1}$ (Garbe et al., 2015). The tomographic scan consisted of a total of 1000 equally spaced angle shadow-radiographs obtained every 0.18° as the sample was rotated 180° about its vertical axis, which

was positioned 20 mm from the detector face. Both dark (closed shutter) and beam profile (open shutter) images were obtained for calibration before initiating shadow-radiograph acquisition. To reduce anomalous noise, a total of four individual radiographs with an exposure length of 15 s were acquired at each angle (Mays et al., 2017). Total scan time was 18 hours.

Neutron activation of the specimen was measured by surface contact using an appropriate hand-held dosimeter, 1 h upon completion of the scan, at 3 days, and one week post-scan. The recordings were 35, 3 and 0 Sv/h respectively. At 2.5 weeks post-scan, no detectable counts per second above background were recorded; the specimen was issued a radiation clearance certificate and cleared for return to the authors.

The individual radiographs were summed in post-acquisition processing using the Grouped ZProjector function, and anomalous white-spots removed using a threshold filter in ImageJ v.1.51h. Normalisation and tomographic reconstruction of the 16-bit raw data were performed using Octopus Reconstruction v.8.8 (Inside Matters NV), yielding virtual slices perpendicular to



the rotation axis. Once the scanned specimen was available, the obtained images were first refined using ImageJ and then inputted into Avizo Lite for segmentation. Figures were then assembled in Adobe Photoshop Elements 8.0 and Adobe Illustrator. The phylogenetic analysis conducted in this study follows the methodology of Rowe et al. (2023), with the analysis performed in PAUP 4.0a169 and the matrix updated in Mesquite.

The electronic version of this article in Portable Document Format (PDF) will represent a published work according to the International Commission on Zoological Nomenclature (ICZN), and hence the new names contained in the electronic version are effectively published under that Code from the electronic edition alone. This published work and the nomenclatural acts it contains have been registered in ZooBank, the online registration system for the ICZN. The ZooBank LSIDs (Life Science Identifiers) can be resolved and the associated information viewed through any standard web browser by appending the LSID to the prefix http://zoobank.org/. The LSID for this publication is: urn:lsid:zoobank.org:pub:20C50EBB-182E-4A9D-9559-4F518034AFBB. The online version of this work is archived and available from the following

112113

103

104

105 106

107

108

109

110111

114 SYSTEMATIC PALEONTOLOGY:

digital repositories: PeerJ, PubMed Central SCIE and CLOCKSS.

- 115 Clade Parareptilia Olson, 1947
- 116 Node **Ankyramorpha** deBraga & Rieppel, 1996
- 117 Superfamily Lanthanosuchoidea Ivachnenko, 1980
- 118 Family **Acleistorhinidae** Daly, 1969
- 119 Genus Klastomycter gen. nov.
- 120 Species conodentatus sp. nov.

121

- 122 Diagnostic Features: Parareptile characterized by the following apomorphies: presence of
- conical homodont dentition which is slightly recurved apically, and presence of a sphenethmoid
- with pronounced medial curvature of the dorsal processes. Can be distinguished from
- 125 Colobomycter by the the presence of a shallowly concave lateral skull margin and four
- premaxillary teeth, a nearly straight nasal-frontal suture, a wide contribution of the postorbital to
- the temporal fenestra. Differs from *Delorhynchus* by the fewer number of maxillary teeth, a
- triradiate jugal; absence of tuberosities on the dorsal skull roof excluding the orbital region,
- absence of an anterolateral palatine process, and an open orbitonasal foramen. Can be
- distinguished from *Acleistorhinus* by the presence of a straight posterior orbital margin, a pointed
- anterior process of the quadratojugal, an enlarged vomerine tooth, a tooth field extending to the
- 132 lateral margin of the palatine, and an extension of the palatal process of the pterygoid reaching to
- the middle of the vomer.

134 **Description**

- 135 General cranial and postcranial proportions: The skull of holotype and only known specimen
- is approximately 29.4 mm in length, with an orbital length of 9.0 mm resulting in a ratio of skull
- length to orbital length of 3.25 (Fig. 1, 2).



140 141 **Figure 1: Holotype of** *Klastomycter conodentatus***.** (A) Dorsal, (B) right lateral and (C) left lateral views. Abbreviations: **epi** = epipterygoid, **f** = frontal, **j** = jugal, **la** = lacrimal, **m** = maxilla, **p** = parietal, **pal** = palatine, **pf** = postfrontal, **pm** = premaxilla, **po** = postorbital, **prf** = prefrontal, **pt** = pterygoid, **qj** = quadratojugal, **sph** = sphenethmoid.

142143144

145

Figure 2: *Klastomycter conodentatus* **in ventral view.** (A) Full specimen in ventral view and (B) ventral skull roof. Abbreviations: **epi** = epipterygoid, **pal** = palatine, **pt** = pterygoid, **qj** = quadratojugal, **sph** = sphenethmoid, **v** = vomer.

146147148

149

150

151

152

153154

155

156

157

158

159

160

161

162

163

164

165

166

167

168

169 170

171

172

173

Skull Roof: In this specimen the left premaxilla is completely preserved, albeit disarticulated, while the right premaxilla is only present as a thin fragment of the dorsal process articulating with the nasal (Fig. 3). The premaxilla is slender rather than broad, with the angle between the midline of the premaxilla and the lateral edge being smaller than that of other comparable species, indicative of an unusually narrow snout. Anteriorly, the rostral end of the premaxilla is rounded in a similar fashion to that of *Acleistorhinus pteroticus* rather than the pointed condition of Colobomycter pholeter (deBraga & Reisz, 1996; MacDougall et al., 2017b). The premaxilla has a thin, curved dorsal process which would connect to the nasal to form the medial border of the external nares. Compared to A. pteroticus, the dorsal process is slender and more closely resembles the condition of C. pholeter. Anteriorly, the base of the dorsal process possesses a small indentation, which may have been a foramen for a premaxillary nerve canal. The tip of the dorsal process has a small groove on its lateral surface, which would have most likely connected to the nasal. Dorsally, the premaxilla is V-shaped with a palatal process projecting posteromedially that is half the length of the premaxillary contribution to the alveolar margin. This palatal process is fairly robust, with a bifurcated tip that would have most likely contacted the anterior vomer. The alveolar margin possesses the same sutural surfaces for the maxilla and septomaxilla as C. pholeter. There are four tooth positions on the right premaxilla of this species, as in Acleistorhinus. Unfortunately, the tooth belonging to the first position is missing. but by the size of the remaining cavity it can be inferred that it was approximately the same size as the second tooth. This cavity suggests that the tooth was somewhat larger than the teeth occupying the maxilla, although not as exaggerated as the fangs seen in C. pholeter (MacDougall et al., 2017b). The slightly larger size of the premaxillary teeth compared to the maxillary teeth differs from what is seen in A. pteroticus in which the largest tooth present is present on the maxilla (deBraga & Reisz, 1996). Each of the three premaxillary teeth which have been preserved in this specimen are conical and compressed in shape with little to no recurvature. The shape and number of premaxillary teeth are poorly known in acleistorhinids, only the holotype of Acleistorhinus has this part of the snout preserved.

174 175 176

Figure 3: Right premaxilla of *Klastomycter conodentatus*, (A) Medial view, (B) ventral view and (C), lateral view.

177 178 179

180

181 182

183

Both elements of the maxilla are present, and it remains in proximity with almost all the surrounding skull roof elements (Fig. 1B, 1C). This dentigerous element is mostly complete on both sides, with the exception of the right premaxillary process. The overall morphology of the maxilla closely resembles *Delorhynchus cifellii* (Reisz, Macdougall & Modesto, 2014), although the anterior portion of the dorsal process connects directly to the nasal instead of the anterior part



212213

214

215216

217

218

219220

221

222

223

224225

226

227228

of the lacrimal exposure. The anterior part of the maxilla possesses several supralabial foramina, 184 the largest of which is the anterolateral maxillary foramen (Reisz at al., 2014). This increased 185 size of the anterolateral maxillary foramen, compared to other maxillary foramina, is a shared 186 187 trait among parareptiles (deBraga & Reisz, 1996). The preserved premaxillary process in this specimen closely resembles the morphology of *Delorhynchus*, while in *Colobomycter* and 188 Acleistorhinus it is more robust. As with other acleistorhinids, the maxillary portion of the 189 external nares is bordered ventrally by the premaxillary process and posteriorly by the dorsal 190 191 lamina. The dorsal lamina of the maxilla in the current specimen is semirectangular, whereas in Acleistorhinus the dorsal process is rounded (deBraga & Reisz, 1996). While not as prominent as 192 in Delorhynchus, an anterodorsal projection of the dorsal lamina contributes to the posterodorsal 193 194 part of the external nares. Several wide, shallow pits are located on the dorsolateral region of the dorsal lamina as a form of skull ornamentation. These pits are also scattered on the lateral 195 surfaces of all other preserved elements of the skull roof excluding the quadratojugal. In 196 comparison to other acleistorhinids, *Klastomycter* lacks pronounced tuberosities on the dorsal 197 skull roof which matches the original description of Acleistorhinus (Daly, 1969). This specimen 198 has nineteen tooth positions on each maxilla. The overall number of tooth positions therefore 199 200 resembles Acleistorhinus most closely, which possesses seventeen teeth on each maxillary 201 element (deBraga & Reisz, 1996). In contrast, D. cifellii possesses twenty-four maxillary tooth positions, while C. pholeter has only thirteen tooth positions due to its enlarged caniniform teeth 202 203 (Reisz, Macdougall & Modesto, 2014; MacDougall et al., 2017). The anterior maxilla has a tall 204 dorsal process which forms the posterior margin of the external nares and connects dorsally to the nasal, lacrimal and prefrontal, similar to what is seen in both *Delorhynchus* and 205 206 Colobomycter. Posteriorly, the maxilla contributes to the ventral margin of the orbits and extend past their posterior margin, terminating in a thin triangular process. Based on morphology of the 207 jugal and quadratojugal, the posterior end of the maxilla would form a point contact with the 208 209 quadratojugal. In contrast to what is seen in Acleistorhinus, the tooth bearing region of the maxilla does not extend past the posterior orbital margin (deBraga & Reisz, 1996). 210

The generally homodont marginal dentition in the present specimen differs from that of *Colobomycter pholeter* and *Acleistorhinus pteroticus* in that this species has much smaller, more uniformly shaped teeth. As in *Delorhynchus cifellii*, this species does not have pronounced caniniform teeth. The premaxillary teeth are the largest of the marginal dentition, followed closely by the maxillary teeth occupying positions 1-4. After this point, the teeth slightly shrink in size with slightly larger teeth reappearing to occupy positions 7-10. The teeth are conical and compressed with only a very slight amount of recurvature. The tips of the teeth form a sharp point as opposed to the more rounded condition seen in *D. cifellii* and *A. pteroticus*. This dentition is distinctive in that even the largest teeth are conical in shape rather than tubular. The teeth on this specimen are most reminiscent to that of *D. cifellii* because of the generally homodont dentition, but the conical shape of the teeth seen in this species is unique and differs from that of other acleistorhinids, including *D. cifellii*, *A. pteroticus* and *C. pholeter*.

The anterior portion of the nasal forms the dorsal margin of the external nares and is connected to the anterodorsal process of the maxilla by its ventrolateral edge (Fig 1A, 2B). It is connected dorsolaterally to the prefrontal, dorsally to the frontal and ventrolaterally to the anterior process of the lacrimal. The outline of the nasal forms a quadrangular shape and, as is seen in *Acleistorhinus pteroticus*, the nasal of this specimen is wider posteriorly rather than anteriorly. However, similarly to *A. pteroticus*, the nasal of this species forms a nearly straight



suture with the frontal, rather than a jagged suture as is seen in *Colobomycter pholeter* and *Delorhynchus cifellii*.

The lacrimal has a long anterior process which lays on the medial surface of the dorsal process of the maxilla and meets the ventrolateral edge of the nasal (Fig. 1B, 1C). This anterior process is partially hidden in lateral view, in contrast to the more exposed anterior process seen in *Delorhynchus cifellii*. In addition, the anterior process terminates at the posterolateral corner of the nasal, instead of the partial separation found in D. cifellii (Reisz et al., 2014). The lateral surface of the lacrimal is bordered ventrally by the maxilla, anteriorly by the posterodorsal process of the maxilla and dorsally by the prefrontal and nasal. The posterolateral exposure of the lacrimal is semilunar in shape and makes up the anteroventral corner of the orbit (Figure 3C), which is bordered dorsally and medially by the prefrontal. Posteroventrally, the lacrimal also has an elongated, thin process which lays against the medial surface of the maxilla and is not visible in lateral view. This thin process ends in a point contact with the anterior process of the jugal much like what is seen in D. cifellii and Colobomycter pholeter. In contrast, A. pteroticus has a more substantial contact between the lacrimal and jugal (deBraga & Reisz, 1996). Posteriorly, there are two foramina on the posterior surface of each lacrimal, with the more dorsal foramen being larger than the ventral foramen. These foramina differ from what is seen in D. cifellii, where the ventral foramen is larger than the dorsal foramen.

While parts of the prefrontal are missing in this specimen, the dorsal and posterior regions are still preserved (Fig. 1). The dorsal face of the prefrontal connects medially to the frontal, anteromedially to the nasal, anterolaterally to the posterior of the dorsal process of the maxilla and laterally to the lacrimal. Anteriorly, the dorsal surface of the prefrontal is thin and tapered like in *Delorhynchus cifellii*, unlike the wide anterior prefrontal seen in *Acleistorhinus pteroticus* (deBraga & Reisz, 1996; Reisz at al., 2014). The posterior surface of the prefrontal makes up the anterior orbit and the anterior first third of the dorsal orbit. Much of this posterior surface sits along the medial surface of the dorsal lacrimal, and these two elements makes up the entire anterior orbit. A thin antorobital wall projects from the ventral surface of the prefrontal, suturing onto the lacrimal as in *Colobomycter pholeter* and *C. vaughni* with the contribution of the prefrontal resembling the latter more closely (MacDougall et al., 2016; MacDougall et al., 2017).

Most of the frontal is preserved in *Klastomycter conodentatus*, with only the anterior portion of the left frontal missing. This element comprises a large portion of the skull roof, connecting anteriorly with the nasal, anterolaterally with the prefrontal, posterolaterally with the postfrontal and posteriorly with the parietal (Figure 1A). The frontal possesses lateral transverse flanges which make up approximately one third of the dorsal orbit and separate the prefrontal and postfrontal bones. Compared to *Acleistorhinus pteroticus*, the frontal of this species extends farther posteriorly and are more alike to the condition seen in *Delorhynchus cifellii* and *Colobomycter pholeter* (deBraga & Reisz, 1996). Additionally, as with these two taxa, the frontal of the current specimen forms a slanted, somewhat jagged connection to the parietal. This is different from the straighter yet gently rounded connection seen in *A. pteroticus*. Ventrally, the antorbital ridge continues onto the frontal, decreasing in height posteriorly as in *D. cifellii* (Rowe et al., 2023).

The postfrontal has a triangular outline in dorsal view and is connected medially to the frontal, posteriorly to the parietal and posterolaterally to the postorbital (Figure 1A). Anterolaterally, the slightly curved edge of the postfrontal comprises the posterior third of the dorsal orbit. The postfrontal of the current specimen does not extend posteriorly, and rather than wedging between the parietal and postorbital as in *Acleistorhinus pteroticus* it terminates just



before the connection between these two elements (deBraga & Reisz, 1996). This is reminiscent of what is seen in *Colobomycter pholeter* and *Delorhynchus cifellii* but with less jagged sutures than that of the latter.

The jugal is a triradiate element connected anteriorly to the lacrimal, ventrally to the maxilla, dorsally to the postorbital and likely posteroventrally to the quadratojugal (Fig. 1B, 1C). The anterodorsal edge of the jugal forms the posterior two thirds of the ventral orbit and part of the posterior orbit. Much like *Acleistorhinus pteroticus* and *Colobomycter pholeter*, the triradiate shape of the preserved jugal confirms that this parareptile had a single lateral temporal fenestra on either side of the skull. However, the reduced dorsal process of the jugal as compared to *A. pteroticus* suggests that the lateral temporal fenestrae were bordered by the jugal, postorbital, squamosal and quadratojugal, as is seen in *Delorhynchus cifellii* and *C. pholeter*. If the dorsal process were taller, as in *A. pteroticus*, the postorbital would not be included in the border of the lateral temporal fenestrae. More support for this idea comes from the fact that the jugal of this specimen is most similar to that of *C. pholeter*, where a single lateral temporal fenestra is bordered by these four elements. Unfortunately, because the squamosal was not preserved in this specimen, its contribution to the temporal fenestra is not certain. Medially, the jugal has a short ramus which projects towards the midline of the skull, as in *Delorhynchus cifellii* (Rowe et al., 2023.

Some damage has occurred to each side of the postorbital but their contribution to the ventral and posterior orbit is still evident (Fig. 1). The postorbital is connected ventrally to the jugal, dorsally to the parietal and anterodorsally to the prefrontal. If the squamosal were preserved, the postorbital would likely be connected to it by the posterior end of its ventral edge, as is seen in *Colobomycter pholeter* and *Delorhynchus cifellii*. This differs significantly from *Acleistorhinus pteroticus*, in which the postorbital does not contact the parietal as it is separated from this element by the postfrontal and supratemporal. Additionally, the similarity of the postorbital morphology to *C. pholeter* suggests that it contributed to the border of the lateral temporal fenestrae. and the squamosal likely did not wrap around the ventral edge of the postorbital to connect to the jugal. This would prevent this element from contributing to the lateral temporal fenestra as is seen in *Acleistorhinus pteroticus*.

The parietal is a broad, flat element making up the posterior border of the skull roof. In dorsal view, the anterior portion of the parietal forms a rounded point where it meets with the frontal (Figure 1B). The parietal connects anterolaterally to the prefrontal and laterally to the postorbital, and potentially the supratemporal if it were preserved. The groove on the parietal where the supratemporal would have fit can be clearly seen on the posterolateral portion of the element, and suggests that the bone was large, as in other acleistorhinids. In this species, the pineal foramen is in the middle of the two parietal elements. This can be contrasted to *Acleistorhinus pteroticus*, in which the pineal foramen is displaced anteriorly, closer to the frontoparietal suture. The condition displayed here is common to both *Colobomycter pholeter* and *Delorhynchus cifellii* and is believed to be the primitive condition of the trait (deBraga & Reisz, 1996). The shallow dimpling present on all skull roof elements is concentrated around the pineal foramen.

While the left quadratojugal is disarticulated, it is still present and complete (Fig. 4). It is likely that this posterior skull roof element contacted the jugal and maxilla anteriorly and the squamosal dorsally. This placement means that the quadratojugal contributed to the ventral and posteroventral margin of the lateral temporal fenestra. The shape of the quadratojugal in this species is very similar to that of *Acleistorhinus pteroticus*, with a concave dorsal edge differing from the condition seen in *Colobomycter pholeter* where the dorsal edge of the quadratojugal



forms a rounded edge. This distinction is important as it indicates that the squamosal in this species likely did not have a ventral process curving around the quadratojugal. Instead, the squamosal likely had a slightly rounded but overall flat dorsal edge which connected with the quadratojugal, as is seen in *Acleistorhinus pteroticus*. Laterally, the quadratojugal is rugose as in *C. pholeter* and *Delorhynchus cifellii* (Macdougall et al., 2014; MacDougall et al., 2017), while lacking the shallow pits seen elsewhere on the skull roof.

327 328

Figure 4: Left quadratojugal of *Klastomycter conodentatus*. (A) Lateral view and (B) medial view.

329 330 331

332

333

334

335

336 337

Palate & Braincase:

Of the five dentigerous elements noted in other acleistorhinids, only the vomer, palatine and pterygoid have been preserved in this specimen with a significant portion of the ventral surface covered by tooth fields (Fig. 5). Ventrolaterally, the choana extends through the palatine and the pterygoid, and would most likely extend through the ectopterygoid as in *Delorhynchus cifellii* (Rowe et al., 2023). However, the channel of the choana is separated from the dentigerous portion of the palatine by a thin ridge.

338 339

Figure 5: Right palate of *Klastomycter conodentatus*. (A) Dorsal view, (B) lateral view and (C) ventral view. Abbreviations: epi = epipterygoid, pal = palatine, pt = pterygoid, v = vomer.

341342

343

344

345 346

347

348

349 350

351

352 353

354

355

356

357

358 359

360

361

340

In palatal view, the vomer is an elongate triangular element (Fig. 5). Posteriorly, the vomer increases in width before narrowing as it wedges between the palatine and pterygoid. The vomer is connected by the posterior portion of its medial edge to the pterygoid and by its posterolateral edge to the palatine. If the paired vomer elements were present, the two would likely meet anteriorly along their medial edge, forming the anterior midline of the palate. The posterior medial edge of the vomer would be separated from its pair by the anterior tip of the pterygoid. The anterior vomer is angled ventrally, as can be seen in lateral view. More than half of the ventral surface of the vomer is covered in teeth. The largest tooth occupies the anteriormost tip of the vomer, a condition shared by *Delorhynchus cifellii* and *Colobomycter pholeter*, and is the largest tooth on the palatal surface. Behind the enlarged tooth is a field of teeth located medially which spans the length of this element. This tooth field extends onto the pterygoid and is three teeth wide at its widest extent. The vomer of the current specimen shows similarities to that of C. pholeter, Acleistorhinus pteroticus and D. cifellii in terms of its triangular shape. However, the tooth fields in this specimen closely resemble D. cifellii, and are distinct from C. pholeter and A. pteroticus (deBraga & Reisz, 1996; Modesto & Reisz, 2008; Rowe et al., 2023). On its dorsal surface, the vomer possesses an alar flange extending posterolaterally onto the palatine towards the anterior edge of the posterior external nares. The vomer is slightly disarticulated here, as it would connect to the orbitonasal ridge of the palatine and form the medial wall of the choana as in D. cifellii. However, the alar flange is comparatively more delicate in Klastomycter conodentatus (Rowe et al., 2023).

362363364

365

366

The palatine is a quadrangular element which connects anteriorly to the vomer and medially to the pterygoid (Fig. 5). In full articulation, it would also connect laterally to the maxilla and dorsally to the lacrimal and prefrontal. One large tooth field occupies the palatine, starting approximately one third from the anteriormost end at the mediolateral midline of the element and continuing posteromedially across it. This diagonal tooth field then continues across the



posteromedial corner of the palatine and continues on to the pterygoid. The anterior end of this tooth field starts as what appears to be a single tooth row, widening to accommodate up to three rows before reducing to two rows on the pterygoid. This differs from *Acleistorhinus pteroticus* in that this tooth field continues farther anteroventrally onto the palatine in *Klastomycter conodentatus*, and the tooth field accommodates three rows of teeth rather than two. Compared to *Delorhynchus cifellii*, the palatine of *K. conodentatus* has a smaller concentration of teeth. In contrast to the condition in *K. conodentatus*, in *Colobomycter pholeter*, the pterygopalatal tooth field is focused more on the palatine rather than on the pterygoid, and becomes larger as it extends onto the pterygoid. The dorsal surface of the palatine possesses an orbitonasal ridge extending laterally towards the posterior edge of the posterior external nares. Comparisons to *A. pteroticus* and *C. pholeter* are not currently possible, but *D. cifellii* possesses a similar set of dorsal ridges. The orbitonasal ridge is open dorsally, unlike *D. cifellii*, where the orbitonasal ridge is enclosed. In addition, unlike the condition in *D. cifellii* and *C. pholeter*, there is no anterolateral process of the palatine that would border the choana laterally (MacDougall et al., 2017; Rowe et al., 2023).

As with many other early Permian amniotes, the pterygoid is a large triangular element composed of an elongated palatal process, a wide transverse process and a posterior quadrate ramus (Fig. 5A, 5C). The palatal process of the pterygoid borders the posteromedial edge of the vomer anteriorly and terminates in a sharp point, and contacts the palatine laterally. There are three distinct tooth fields on the ventral surface of the palatal process, with the first tooth field originating at the posteromedial corner of the palatal process and continuing anteriorly along the medial border of the pterygoid. This tooth field becomes smaller in both the number of tooth rows and the size of individual teeth until it disappear entirely about halfway along the medial edge of the palatal process. The second tooth field on the palatal process of the pterygoid continues onto the pterygoid from the vomer, located along the longitudinal axis of the palatal process of the pterygoid and disappearing about a third of the way from the posterior edge of this element. The last tooth field located on the ventral surface of the pterygoid is a continuation of the tooth field of the palatine and is composed of two rows of teeth that extend diagonally across the pterygoid before terminating just before the quadrate ramus. The locations of the tooth fields on the palatal process of the pterygoid are similar to that seen in Acleistorhinus pteroticus but the fields themselves are much larger, consisting of more rows of teeth and larger teeth. Overall, the tooth fields on the current specimen take up a larger proportion of the ventral surface area of the pterygoid than in A. pteroticus. This condition also differs from that seen in Colobomycter pholeter and Delorhynchus cifellii as the teeth occupying this region in these species seem to be more numerous vet more spread out.

The transverse process of the pterygoid extends ventroposterolaterally from the posterolateral edge of the palatal process of the pterygoid. In ventral view the transverse process is triangular in shape, and nearly the entirety of the ventral surface of this process is covered in teeth. These teeth make up the fourth tooth field present on the pterygoid of this species, bordering the posterior edge of the transverse process and continuing medially onto the raised ventral edge of the quadrate ramus. Laterally, this tooth row wraps around the posterolateral corner of the ventral face of the transverse process. The teeth located on this lateral edge are some of the largest present on the palate, with four teeth on the posterior transverse process that are nearly as large as the single large tooth occupying the anteriormost tip of the vomer. In addition to the distinct row of teeth on the transverse process, there is a large cluster of smaller teeth which cover the rest of the ventral surface of this process. At its widest point, the tooth field on the transverse



 process is made up of five rows of teeth. This tooth field is much larger and wider than that seen in *Acleistorhinus pteroticus*, in addition to the fact that the teeth themselves making up this field are much larger in *Klastomycter conodentatus*. The transverse process of the pterygoid is more similar to that seen in *Colobomycter pholeter* and *Delorhynchus cifellii*.

Posteriorly, the quadrate ramus of the pterygoid is a large semiconical sheet of bone which extends posterodorsally from the posterior edge of the dorsal surface of the palatine process (Fig. 5). As it extends dorsally this process widens into a thin sheet culminating in a dorsal point. In lateral view, this process resembles a wing attached to the posterior end of the dorsal surface of the palate. The morphology of the quadrate ramus is very similar to that of *Delorhynchus cifellii*, but cannot be compared to *Colobomycter pholeter* or *Acleistorhinus pteroticus* due to the current lack of information.

The right epipterygoid has also been preserved in association with this specimen, and is slightly disarticulated from the quadrate ramus of the pterygoid (Figure 5B) This element consists of a ventral footplate which is broad, oval shaped and elongated anteroposteriorly, and a thin dorsal process with modest posterior curvature. The morphology of this element closely resembles the condition of *Delorhynchus cifellii* (Rowe et al., 2023) and indicates the probable presence of a suborbital foramen.

The sphenethmoid is a large, Y-shaped element in anterior and posterior view which has been very well-preserved (Figure 6). In this specimen, it has shifted out of place, but is still relatively close to its articulating position on the ventral surface of the frontal (Figure 3B; Figure 4A). Dorsally, this element bifurcates into two processes curving medially which form the trough of the sphenethmoid (Figure 6) (MacDougall et al., 2019). The morphology of the dorsal processes differs significantly from that seen *Delorhynchus cifellii*, where the dorsal processes do not curve medially (Rowe et al., 2023). While the sphenethmoid of *Colobomycter pholeter* is not fully visible, it appears to possess a more modest curvature than *Klastomycter conodentatus* (Modesto & Reisz, 2008). In *Feeserpeton*, the dorsal processes of the sphenethmoid lack curvature and diverge laterally (MacDougall et al., 2019). The posterior end of the sphenethmoid curves downward into a short lip where the dorsal processes meet. Ventrally, the sphenethmoid has a long, straight, bladelike keel which widens slightly towards its tip. This keel extends anteriorly past the dorsal processes and terminates in a sharp point above the contact between the dorsal processes.

Figure 6: Sphenethmoid of *Klastomycter conodentatus***.** (A) Anterior view, (B) posterior view and (C) left lateral views.

Phylogenetic analysis

In order to determine the relationship of *Klastomycter* to other members of Parareptilia, and acleistorhinids specifically, we included it in the phylogenetic analysis conducted in Rowe et al. (2023). The only change to that matrix was the addition of character states for *Klastomycter*. Given the narrow scale of this study we did not include a broad range of taxa, or compare the results to Ford & Benson (2020) and Simoes et al. (2022). While it is important to evaluate the relationships between Parareptilia and other early amniotes, we do not consider this study to be a suitable place for such an undertaking.

Figure 7: Strict consensus of 14 most parsimonious cladograms of parareptile relationships.



A strict consensus of 14 most parsimonious cladograms of parareptile relationships is displayed as Figure 7. The tree length in a heuristic is 633 steps, with 1000 replicates, and 73882182 rearrangements tried, and has a consistency index (CI) of 0.348, a rescaled consistency index (RC) of 0.564. Homoplasy index (HI) is 0.652, while the RC index is 0.196. Despite some of the more pronounced similarities of *Klastomycter* to *Acleistorhinus*, such as the lack of skull roof tuberosities, this new taxon is resolved as a sister taxon to *Delorhynchus*. Lanthanosuchus and Acleistorhinus form a clade as sister to the other so-called acleistorhinids. while *Feeserpeton* and the clade Bolosauridae are sister taxa to them. This pattern is the same as the previous analysis of parareptile interrelationships, but with *Klastomycter* closely related to Delorhynchus and Colobomycter. However, it must be noted that this pattern of relationship is weakly supported, and it only takes one extra step to collapse most basal parareptilian clades, with the exception of the clade formed by Klastomycter, Delorhynchus, Colobomycter. In view of that weakness, we refrain from changing the higher level designations until a better resolution to the patterns of relationships can be achieved. Thus, the family Acleistorhinidae was erected by Daly in 1969, when the parareptilian identity of *Delorhynchus* (Fox, 1962) and *Colobomycter* (Vaughn, 1958) were unknown. Similarly, the order and family designation of Lanthanosuchoidea (Efremov, 1946) was erected when the Acleistorhinidae were unknown.

Conclusions

Acleistorhinid diversity at the Richards Spur locality has continued to expand with the addition of this new taxon. Much of the diversity appears to be centered around the dentition, and its effect on the cranial anatomies of these small predators. As previously suggested, the Dolese Brothers Limestone Quarry locality and its cave deposits provide an unprecedented record of fine resource partitioning, with different but closely related taxa apparently using different types of dentition for food capture and possible processing. The latest member of this clade of small predators appears different from other acleistorhinids in the unusual conical shape of the teeth, but otherwise resemble most closely the more commonly found *Delorhynchus*.

In addition to the six acleistorhinid taxa found at this locality, other small parareptiles also show startling dental diversity. Notable among these are three taxa of parareptiles, *Bolosaurus, Microleter*, and *Abyssomedon*. These taxa fall outside Acleistorhinidae, and demonstrate that there was both an early diversification of this clade, and a broader diversity of early parareptiles not normally preserved (with the exception of Bolosauridae) in the Permo-Carboniferous sediments of Laurasia. This absence speaks to the overall limited knowledge of the fossil record of small amniotes in the initial stages of terrestrial vertebrate evolution, and that localities that represent natural traps provide a glimpse of this fundamental part of amniote history.

The Richards Spur locality underscores this lack of information, with the excellent preservation of unusual closely related taxa of small amniotes among the hundreds of thousands of known isolated and fragmentary bones, and the hundreds of skulls, partial skulls, and partial skeletons that have been recently uncovered. The new parareptile described here is a rare element of this community, as are some of the other parareptiles listed above, with *Delorhynchus* and *Colobomycter* being more frequently encountered in recently opened caves in Richards Spur.

This fine level of resource partitioning as recorded at the Richards Spur locality is not restricted to the parareptiles, but is also found among the captorhinid eureptiles, and is unknown elsewhere among Paleozoic terrestrial tetrapod localities. This is in great part because the cave



- deposits here, excavated as part of a large limestone quarry operation for nearly a century,
- represents by far the richest fossil locality for the. The current evidence seems to indicate that
- other members of this paleocommunity preserved at this locality do not duplicate this level of
- taxic diversity, or this level of resource partitioning, although there are a couple of currently
- recognized small recumbirostran microsaurs. Similarly, the larger dissorophids are currently
- represented by three taxa, while trematopids appear to be restricted to a single taxon. New,
- ongoing research is likely to change this pattern, as new taxa are expected to be uncovered and
- 512 incorporated into the expanding knowledge of this unique early Permian terrestrial tetrapod
- 513 community.

Acknowledgements

- We would like to acknowledge the staff of the Burpee Museum of Natural History for the loan of
- 517 this specimen, and Ms. D. Scott for preparation and assistance with anatomy. We also
- acknowledge E. Beauchesne for her invaluable assistance with preparation of the scanned
- 519 specimen.

520 521

Funding

- 522 This study was made possible by funding from the University of Toronto, Jilin University and a
- Natural Sciences and Engineering Research Council Discovery Grant (RGPIN-2020-04959) to
- Robert R. Reisz. The funders had no role in study design, data collection and analysis, decision
- 525 to publish or preparation of the manuscript.

526 527

References

- 528 Daly, E. (1969). A New Procolophonid Reptile from the Lower Permian of Oklahoma. *Journal*
- of Vertebrate Paleontology, 43(3), 676-687. https://www.jstor.org/stable/1302462
- deBraga, M., & Reisz, R. R. (1996). The early Permian reptile Acleistorhinus pteroticus and its
- phylogenetic position. *Journal of Vertebrate Paleontology*, 16(3), 384–395.
- 532 https://doi.org/10.1080/02724634.1996.10011328
- 533 Efremov, J. A. 1946. [On the subclass of the Batrachosauria, a group of forms intermediate
- between amphibians and reptiles]. Izvestia Biological Division of Sciences, Academy of Sciences
- 535 *USSRR 6*, 616–638. [Russian]
- Garbe, U., Randall, T., Hughes, C., Davidson, G., Pangelis, S., & Kennedy, S. J. (2015). A New
- Neutron Radiography / Tomography / Imaging Station DINGO at OPAL. *Physics Procedia* 69,
- 538 27–32. https://doi.org/10.1016/j.phpro.2015.07.003
- Haridy, Y., Macdougall, M. J., Scott, D., & Reisz, R. R. (2016). Ontogenetic change in the
- 540 temporal region of the Early Permian parareptile *Delorhynchus cifellii* and the implications for
- closure of the temporal fenestra in amniotes. *PLoS ONE*, 11(12).
- 542 https://doi.org/10.1371/journal.pone.0166819
- MacDougall, M. J. & Reisz, R. R. (2012). A new parareptile (Parareptilia, Lanthanosuchoidea)
- from the Early Permian of Oklahoma. *Journal of Vertebrate Paleontology*, 32(5), 1018-1026.
- 545 https://doi.org/10.1080/02724634.2012.679757
- MacDougall, M. J., Scott, D., Modesto, S. P., Williams, S. A., & Reisz, R. R. (2017). New
- 547 material of the reptile *Colobomycter pholeter* (Parareptilia: Lanthanosuchoidea) and the diversity

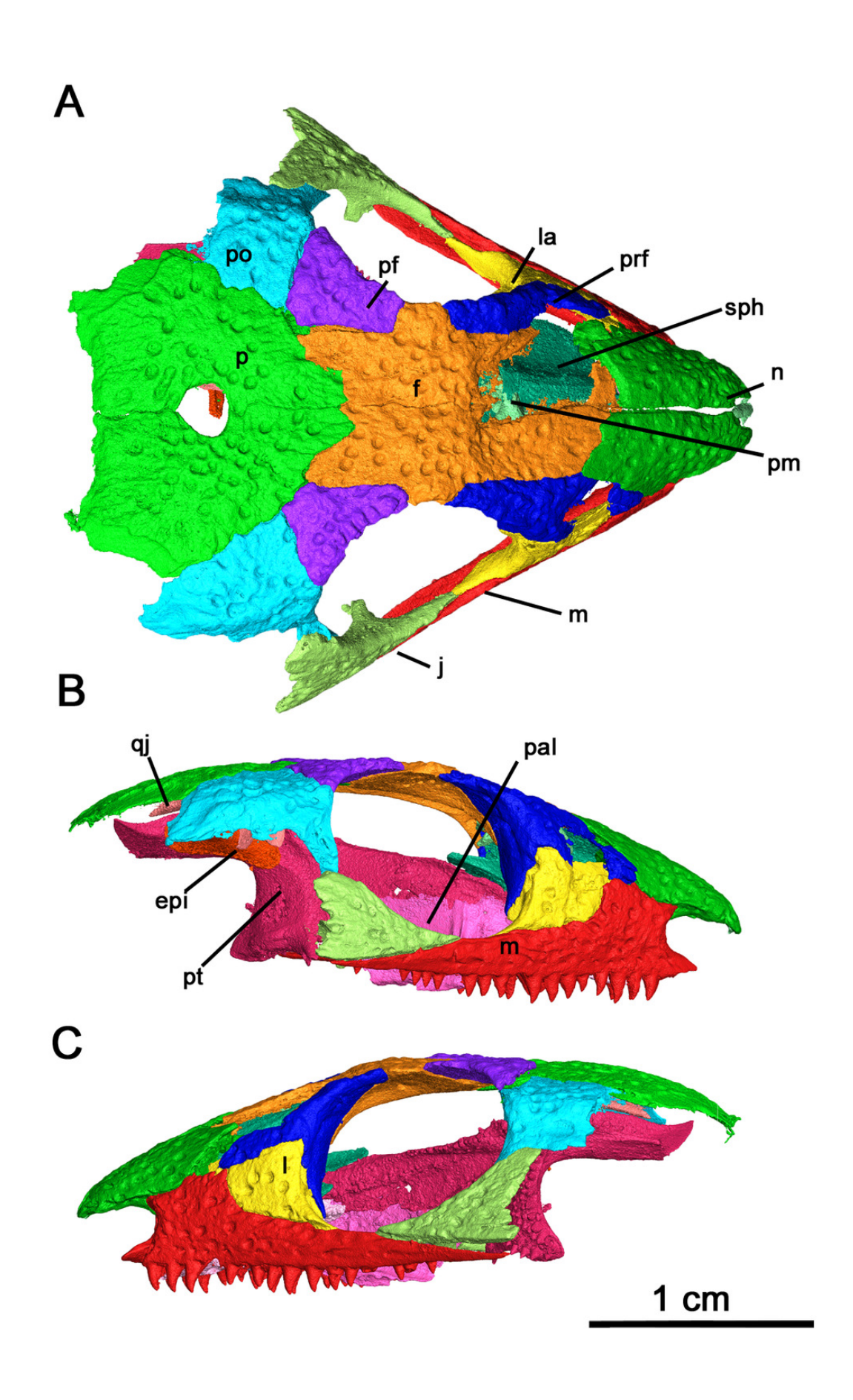


- of reptiles during the Early Permian (Cisuralian). Zoological Journal of the Linnean Society,
- 549 *180*(3), 661–671. https://doi.org/10.1093/zoolinnean/zlw012
- 550 MacDougall, M. J., Tabor, N. J., Woodhead, J., Daoust, A. R. & Reisz, R. R. (2017). The unique
- preservational environment of the Early Permian (Cisuralian) fossiliferous cave deposits of the
- Richards Spur locality, Oklahoma. Paleogeography, Paleoclimatology, Palaeoecology, 475
- 553 (2017), 1-11. https://doi.org/10.1016/j.palaeo.2017.02.019
- MacDougall, M. J., Winge, A., Ponstein, J., Jansen, M., Reisz, R. R., & Fröbisch, J. (2019). New
- information on the early Permian lanthanosuchoid Feeserpeton oklahomensis based on computed
- tomography. *PeerJ*. https://doi.org/10.7717/peerj.7753
- Mays, C., Bevitt, J., & Stilwell, J. (2017) Pushing the limits of neutron tomography in
- 558 palaeontology: Three-dimensional modelling of in situ resin within fossil plants, Palaeontologia
- 559 Electronica 20: 1-12
- Modesto, S. P., & Reisz, R. R. (2008). New material of *Colobomycter pholeter*, a small
- parareptile from the lower permian of Oklahoma. Journal of Vertebrate Paleontology, 28(3),
- 562 677–684. https://doi.org/10.1671/0272-4634(2008)28[677:NMOCPA]2.0.CO;2
- Olson, E. C. (1991). An eryopid (Amphibia: Labyrinthodontia) from the fort sill fissures, Lower
- Permian, Oklahoma. Journal of Vertebrate Paleontology, 11(1), 130–132.
- 565 https://doi.org/10.1080/02724634.1991.10011379
- Reisz, R. R., Barkas, V., & Scott, D. (2002). A new early permian bolosaurid reptile from the
- 567 richards spur dolese brothers quarry, near fort sill, Oklahoma. Journal of Vertebrate
- 568 *Paleontology*, 22(1), 23–28. https://doi.org/10.1671/0272-
- 569 4634(2002)022[0023:ANEPBR]2.0.CO;2
- Reisz, R. R., Macdougall, M. J., & Modesto, S. P. (2014). A new species of the parareptile genus
- 571 Delorhynchus, based on articulated skeletal remains from Richards Spur, Lower Permian of
- 572 Oklahoma. Journal of Vertebrate Paleontology, 34(5), 1033–1043.
- 573 https://doi.org/10.1080/02724634.2013.829844
- Rowe, D. C. T., Scott, D. M., Bevitt, J. J. & Reisz, R. R. (2021). Multiple tooth-rowed
- parareptile from the early Permian of Oklahoma. Frontiers in Earth Science, 9:709497.
- 576 https://doi.org/10.3389/feart.2021.709497
- Rowe, D. C. T., Bevitt, J. J. & Reisz, R. R. (2023). Skeletal anatomy of the early Permian
- 578 parareptile *Delorhynchus* with new information provided by neutron tomography. PeerJ, (zzz)
- 579 Sullivan, C., Reisz, R. R., & May, W. J. (2000). Large dissorophoid skeletal elements from the
- lower permian Richards Spur fissures, Oklahoma, and their paleoecological implications.
- 581 *Journal of Vertebrate Paleontology*, 20(3), 456–461. https://doi.org/10.1671/0272-
- 582 4634(2000)020[0456:LDSEFT]2.0.CO;2
- Tsuji, L. A., Müller, J., & Reisz, R. R. (2010). Microleter mckinzieorum gen. et sp. nov. from the
- lower permian of oklahoma: The basalmost parareptile from laurasia. *Journal of Systematic*
- 585 Palaeontology, 8(2), 245–255. https://doi.org/10.1080/14772010903461099
- Vaughn, P.P. (1958). On a new pelycosaur from the lower Permian of Oklahoma, and on the
- origin of the family Caseidae. *Journal of Paleontology 32: 981–991*.



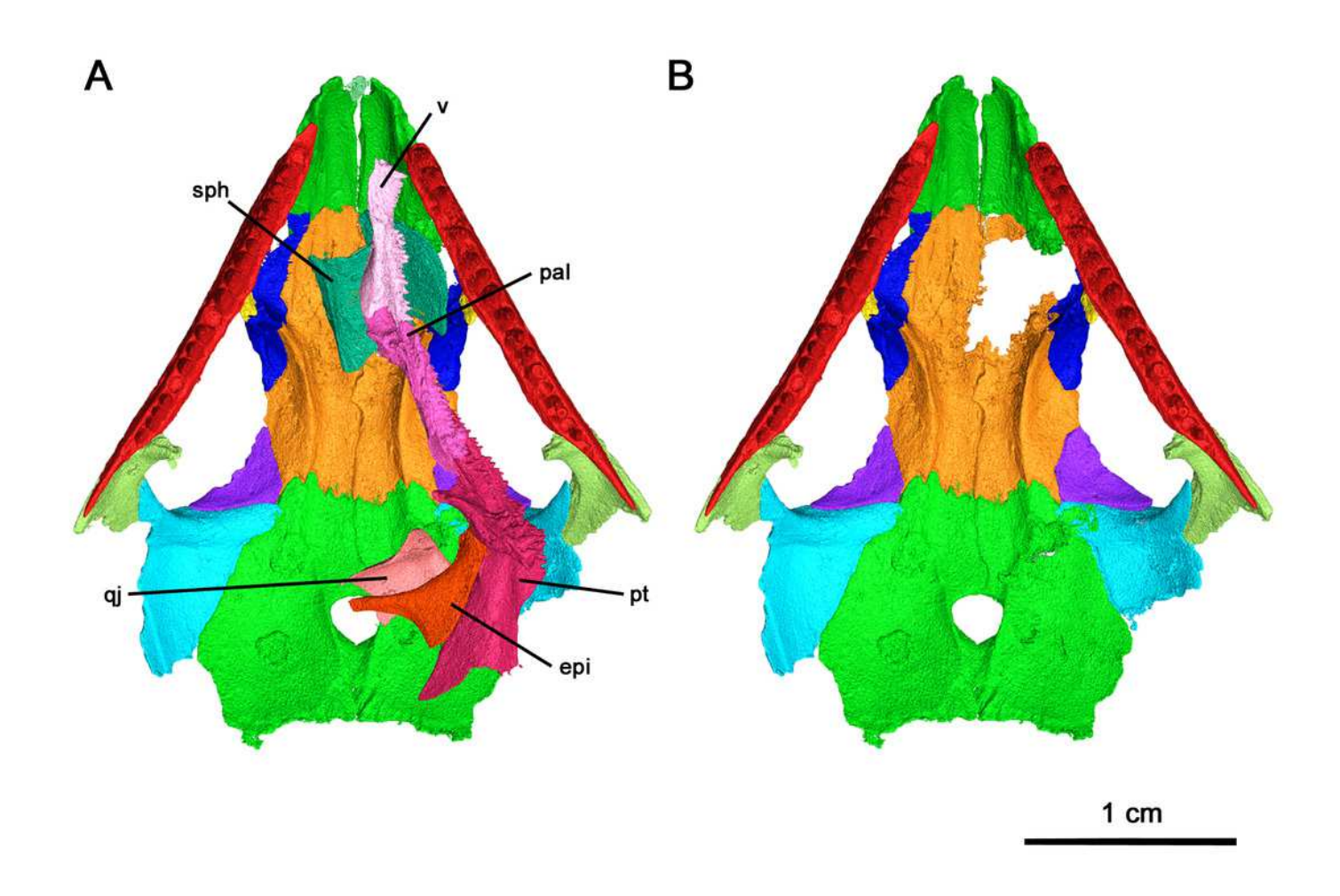
Holotype of Klastomycter conodentatus.

(A) Dorsal, (B) right lateral and (C) left lateral views. Abbreviations: **epi** = epipterygoid, **f** = frontal, **j** = jugal, **la** = lacrimal, **m** = maxilla, **p** = parietal, **pal** = palatine, **pf** = postfrontal, **pm** = premaxilla, **po** = postorbital, **prf** = prefrontal, pt = pterygoid, **qj** = quadratojugal, **sph** = sphenethmoid.



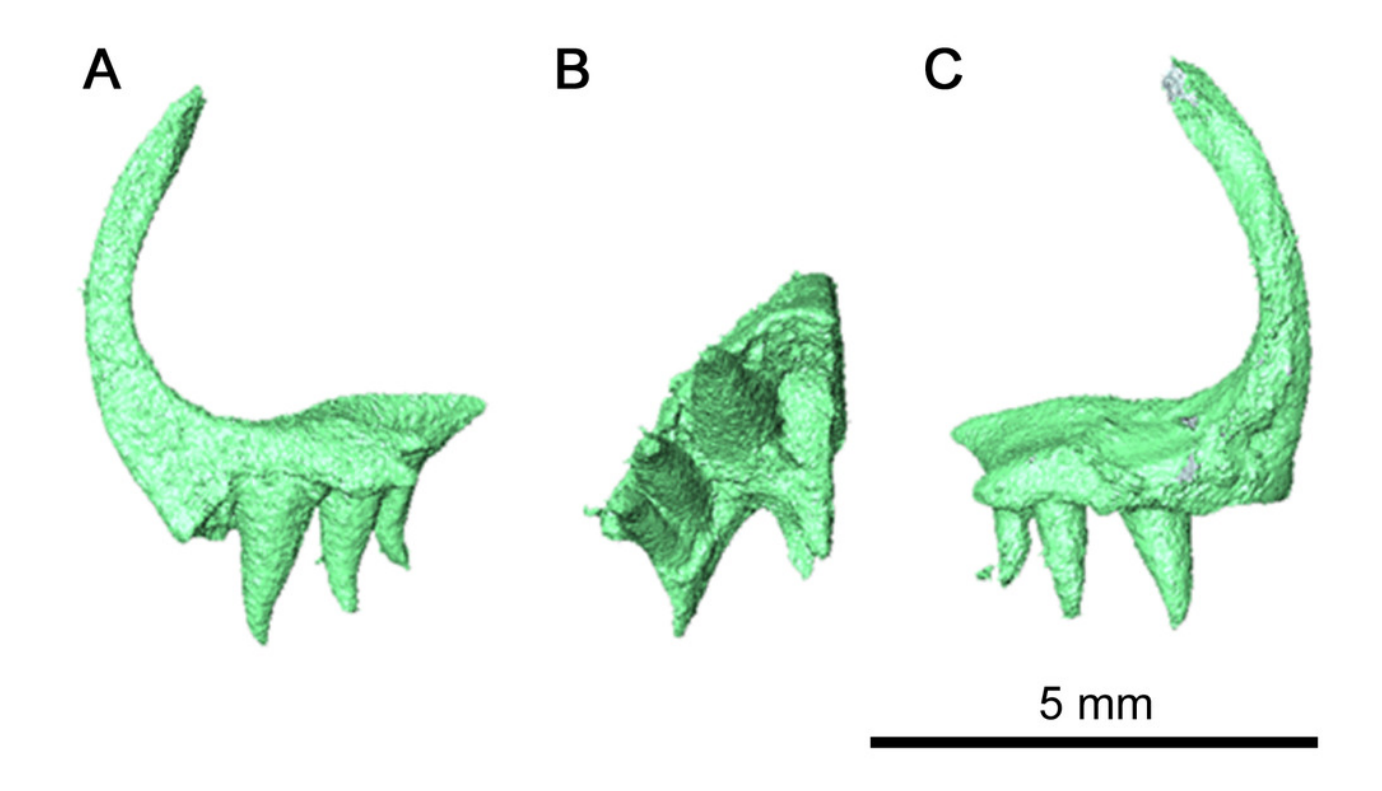
Klastomycter conodentatus in ventral view.

(A) Full specimen in ventral view and (B) ventral skull roof. Abbreviations: **epi** = epipterygoid, **pal** = palatine, **pt** = pterygoid, **qj** = quadratojugal, **sph** = sphenethmoid, **v** = vomer.



Right premaxilla of Klastomycter conodentatus.

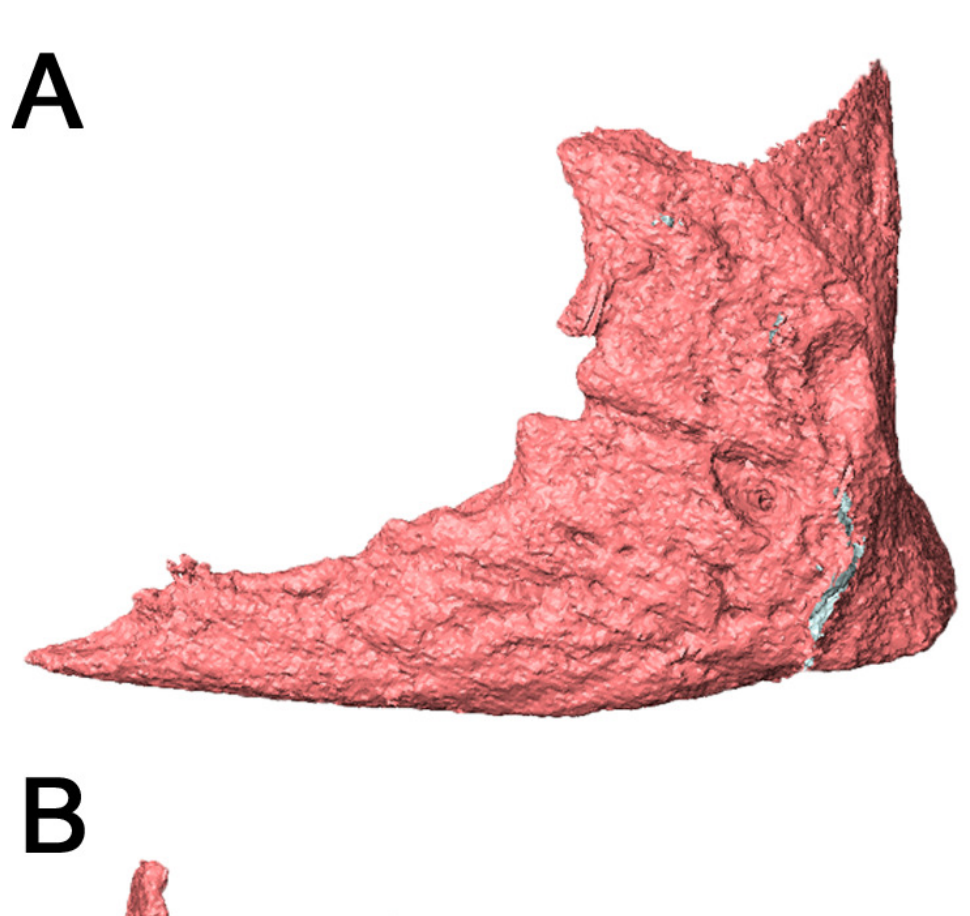
(A) Medial view, (B) ventral view and (C), lateral view.

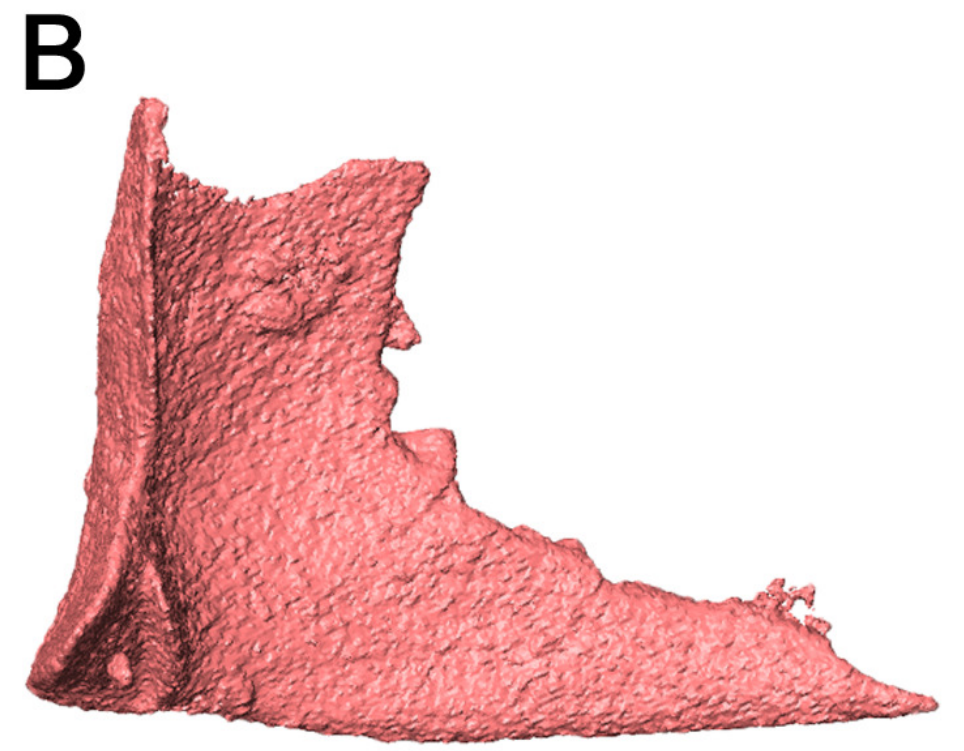




Left quadratojugal of Klastomycter conodentatus.

(A) Lateral view and (B) medial view.



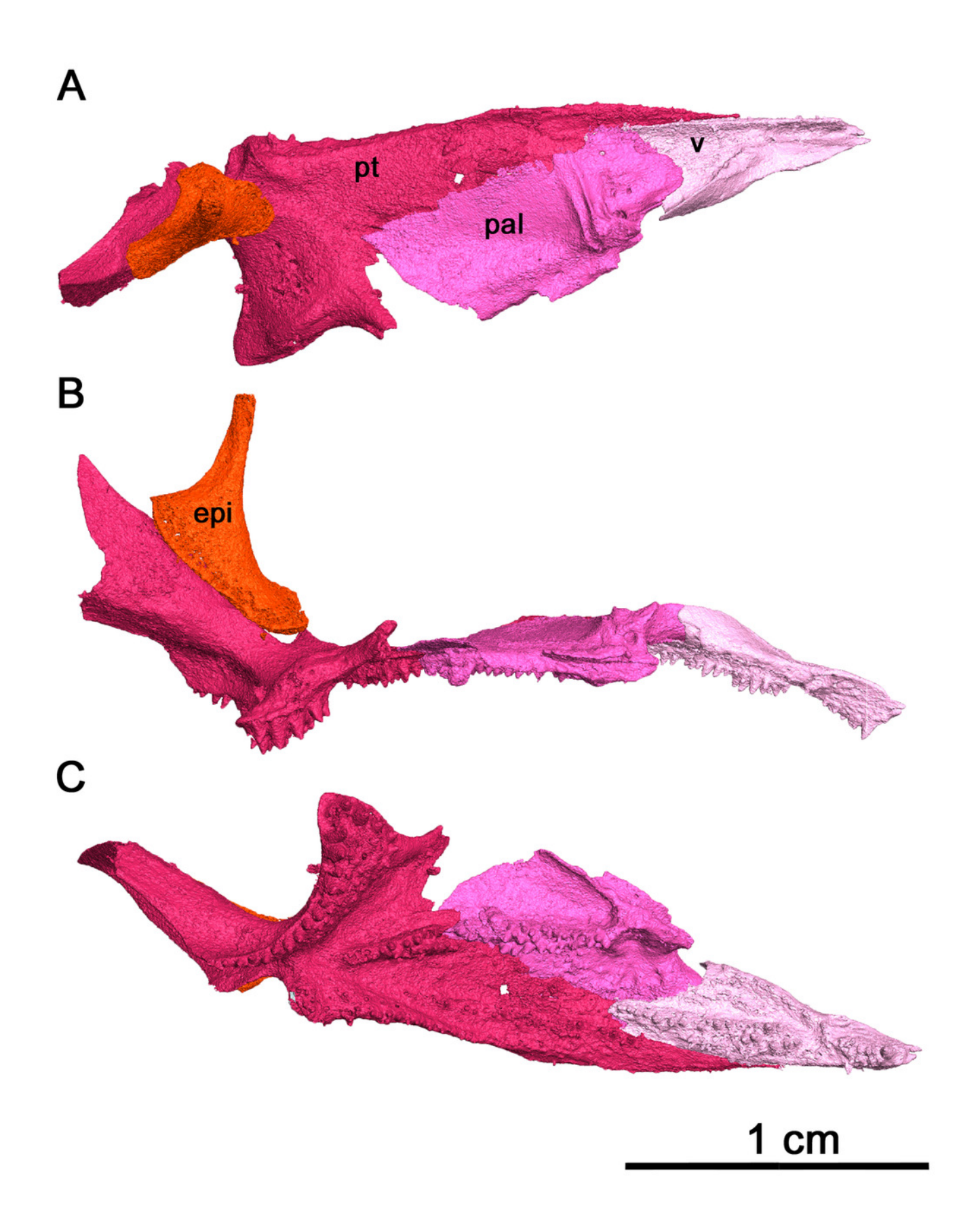


5 mm



Right palate of *Klastomycter conodentatus*.

(A) Dorsal view, (B) lateral view and (C) ventral view. Abbreviations: **epi** = epipterygoid, **pal** = palatine, **pt** = pterygoid, **v** = vomer.





Sphenethmoid of *Klastomycter conodentatus*.

(A) Anterior view, (B) posterior view and (C) left lateral views.



Strict consensus of 14 most parsimonious cladograms of parareptile relationships.

